Triple-point wetting of van der Waals films on self-affine and mound rough surfaces

G. Palasantzas*
Department of Applied Physics, Materials Science Center, University of Groningen, Nijenborgh 4, 9747 AG Groningen, The Netherlands

G. M. E. A. Backx
Computational Physics Centre, Briljantstraat 341, 9743 NM Groningen, The Netherlands

(Received 26 February 2002; revised manuscript received 15 May 2002; published 26 August 2002)

The influence of random self-affine and mound substrate roughness on the wetting scenario of adsorbed van der Waals films is investigated as a function of characteristic roughness parameters. The roughness influence, which leads to triple-point wetting, is calculated by the bending free energy penalty of a solid film picking up the substrate morphology. For self-affine roughness, an increment of the roughness exponent H and/or a decrement of the roughness ratio w/ξ (with w being the rms roughness amplitude and ξ the in-plane correlation length) leads to a noticeable increment of the thickness of adsorbed solid films. Similarly for mound roughness the thickness dependence of the solid wetting layer on the average mound separation λ and system correlation length ζ follow the general scenario that smoother substrates ($w/\zeta \ll 1$ and/or $w/\lambda \ll 1$) lead to thicker solid films. Nevertheless, in this case the thickness increment is a highly nonmonotonic function of ζ and λ for $\lambda \leqslant \zeta$.

DOI: 10.1103/PhysRevE.66.021604 PACS number(s): 68.08.Bc, 67.70.+n, 64.70.Hz, 68.35.Rh

I. INTRODUCTION

The phenomenon of wetting of solid substrates exposed to a gas (under thermodynamic equilibrium conditions) is a topic of intense research from both the fundamental [1,2] and application [3–5] point of view. The wetting of a substrate by a liquid is driven by the strong substrate/particle (van der Waals) attraction forces. Currently there is a rather clear microscopic understanding of wetting on flat solid substrates [1,2,6]. In this case, the liquid film thickness is described as a function of substrate/particle and interparticle interactions for specified thermodynamic parameters (pressure and temperature). Experiments using noble gases [1] on different substrates confirmed that the thickness of the wetting layer grows with increasing substrate/particle attraction (for fixed thermodynamic parameters), as well as that complete wetting (diverging liquid film thickness) occurs for a stronger substrate/particle attraction than interparticle interactions (and thermodynamic conditions approaching liquid-gas coexistence). The latter occurs for system temperature $T > T_3$ with T_3 the triple temperature. However, when $T < T_3$ a solid film of finite thickness ℓ_s is formed close to the sublimation line.

Experimentally [7–10], it has been proven that the thickness ℓ_s of the solid film is always finite when gas-solid coexistence is approached. Only near the triple point a liquid film on top of the solid film is formed with a thickness that diverges as the triple point is approached leading to the so-called triple-point wetting. A critical difference between solid and liquid wetting stems from the inability of a solid to relax the elastic compression originating by the substrate attraction (incorporated in the reduced wall-particle Hamaker constant R). This difference is the basic ingredient in the Gittes-Schick theory [11] of solid film adsorption on flat substrates. Complete wetting occurs for $R = R_o$, while for $R > R_o$ the solid film thickness ℓ_s decreases with increasing R [11].

At any rate, the GS theory [11] neglects substrate roughness, which is the case of almost all real solid surfaces. Recently it was shown that the key parameter governing adsorption of solid films is the substrate roughness rather than the elastic deformation caused by the substrate attraction [12]. As a result the triple-point wetting originates from and is controlled by substrate roughness. Moreover, it was shown by theory and confirmed by experiment (for hydrogen adsorbed films on Au substrates) that a finite substrate roughness leads inevitably to triple-point wetting, and yields a solid layer thickness ℓ_s that is considerably reduced even for small substrate roughness [12].

So far, however, the former study did not show the direct dependence of the triple-point wetting on characteristic roughness parameters describing random roughness fluctuations at any lateral length scale. Such roughness parameters can be measured by scattering and scanning probe microscopy techniques (i.e., x-ray reflectivity, atomic force microscopy, etc.) [13], yielding the possibility to control wetting phenomena by proper manipulation of the substrate roughness. Notably, for a wide variety of surfaces (i.e., the nanometer scale topology of vapor deposited thin films, eroded, and fractured surfaces, etc.) the associated roughness morphology is quantified in terms of self-affine fractal scaling [13,14]. The latter is characterized by the rms roughness amplitude w, the in-plane correlation length ξ, and the roughness exponent H ($0 < H < 1$) that describes the irregularity of short range ($< \xi$) roughness fluctuations [13,14]. In addition, during epitaxial film growth, the growth front can be rough in the sense that multilayer step structures are formed [15,16]. In this case the existence of an asymmetric step-edge diffusion barrier (the Schwoebel barrier) inhibits the down-hill diffusion of incoming atoms leading effectively to

*Corresponding author. Email address: g.palasantzas@phys.rug.nl

the creation of multilayer step structures in the form of mounds [15,16].

Therefore, in this paper we will present a direct quantitative relation of a triple-point wetting characteristic (i.e., solid layer thickness ℓ_s) as a function of self-affine and mound characteristic roughness parameters which are directly accessible by experiment.

II. WETTING THEORY

For rough solid substrates, the wetting layer thickness for fixed thermodynamic parameters (T and P) is obtained by the minimization of the excess grant canonical free energy $\Sigma(\ell_s,\ell_\ell)=\Sigma_1(\ell_s,\ell_\ell)+\Sigma_2(\ell_s)+\Sigma_3(\ell_s)$ (per unit area) relative to a nonwetting situation [11,12]. This is assumed to be the case for a liquid film of thickness ℓ_ℓ on top of a solid film of thickness ℓ_s, which is on top of the rough solid substrate. $\Sigma_1(\ell_s,\ell_\ell)$ is the thermodynamic part [1,17]; $\Sigma_2(\ell_s)$ is the free energy penalty due to substrate attraction [7,11]; and $\Sigma_3(\ell_s)$ is the elastic free energy due to solid layer bending caused by the substrate roughness. The terms $\Sigma_1(\ell_s,\ell_\ell)$ and $\Sigma_2(\ell_s)$ constitute the GS theory and are given by [11]

$$\Sigma_1(\ell_s,\ell_\ell)=\gamma_{ws}+\gamma_{s\ell}+\gamma_{\ell g}-\gamma_{wg}+\ell_s(P_o-P)\frac{\rho_s}{\rho_g}+\ell_\ell(P_o-P)\frac{\rho_\ell}{\rho_g}+\frac{A_1}{\ell_s^2}+\frac{A_2}{\ell_\ell^2}+\frac{A_3}{(\ell_s+\ell_\ell)^2} \tag{1}$$

$$\Sigma_2(\ell_s)=-\frac{3E}{2(1+v)}S^2(\ell_s^{-1}+S\ell_s^{-2}) \tag{2}$$

with γ's the extrapolated interfacial tensions between wall (w), solid (s), liquid (ℓ), and gas (g). E is Young's modulus of the adsorbed solid film and v its Poisson ratio. P_o and P_o' are the coexistence pressures, respectively, between gas/solid and gas/liquid. ρ_g, ρ_ℓ, and ρ_s are the number densities at gas/solid and gas/liquid coexistence ($\rho_g \ll \rho_\ell < \rho_s$). C and H, respectively, the Hamaker constants of the van der Walls tails of the substrate/particle and particle/particle interaction potentials ($-2C/z^3$ and $-2H/\pi r^6$ for large z and r separations) with $A_1=(\rho_s-\rho_\ell)(C-\rho_s H)$, $A_2=(\rho_s-\rho_\ell)\rho_\ell H$, and $A_3=\rho_\ell(C-\rho_s H)$ [1]. $S=0.0229\ (R-R_o)\sigma$ is the reduced stress with $R=C/H\rho_s$ and σ a molecular length scale [11].

For the term $\Sigma_3(\ell_s)$ we assume the substrate roughness to be described by a single valued random function $h(\vec{r})$ of the in-plane position vector $\vec{r}$ ($\langle h(\vec{r})\rangle=0$) [18]. A weakly bent crystalline layer of width ℓ_s will cost an elastic free energy [12,19]

$$\Sigma_3(\ell_s)=\frac{E\ell_s^3}{24(1-v^2)}G,$$

$$G=\frac{1}{A}\int_A\{(\nabla^2 h)^2+2(1-v)[(\partial_{xy}^2 h)^2-\partial_{xx}^2 h\,\partial_{yy}^2 h]\}d^2\vec{r} \tag{3}$$

with A the average flat macroscopic area. If we define the Fourier transform $h(\vec{r})=\int h(\vec{q})e^{-j\vec{q}\cdot\vec{r}}d^2\vec{q}$ and assume translation invariant roughness or $\langle h(\vec{q})h(\vec{q}')\rangle=[(2\pi)^4/A]\langle|h(\vec{q})|^2\rangle\delta^2(\vec{q}+\vec{q}')$ with $\langle\cdots\rangle$ an ensemble average over possible roughness configurations, we obtain for the roughness factor G in Eq. (3)

$$G=\frac{(2\pi)^4}{A}\int_{0\le|\vec{q}|<Q_c}q^4\langle|h(\vec{q})|^2\rangle d^2\vec{q} \tag{4}$$

with $\langle|h(\vec{q})|^2\rangle$ being the roughness spectrum which is required for the calculation of $\Sigma_3(\ell_s)$, and $Q_c=\pi/c_o$ being an upper roughness cutoff with c_o of the order of atomic dimensions. Roughness effects on the *liquid* part of the wetting layer are much smaller and are thus neglected [20].

III. ROUGHNESS MODELS

Self-affine roughness. For self-affine fractal roughness $\langle|h(\vec{q})|^2\rangle$ scales as a power-law $\langle|h(\vec{q})|^2\rangle\propto q^{-2-2H}$ if $q\xi\gg1$, and $\langle|h(\vec{q})|^2\rangle\propto$const if $q\xi\ll1$ [14]. The roughness exponent H is a measure of the degree of surface irregularity [12], such that small values of H characterize more jagged or irregular surfaces at short length scales ($<\xi$). This scaling behavior is satisfied by the simple Lorentzian form [21]

$$\langle|h(\vec{q})|^2\rangle=\frac{A}{(2\pi)^5}\frac{w^2\xi^2}{(1+aq^2\xi^2)^{1+H}} \tag{5}$$

with $a=(1/2H)[1-(1+aQ_c^2\xi^2)^{-H}]$ for $0<H<1$ (power-law roughness).

Mound Roughness. Mound rough surfaces have been described in the past by the interface width w, the system correlation length ζ that determines how randomly the mounds are distributed on the surface, and the average mound separation λ [16]. Such a rough morphology can be described by the roughness spectrum $\langle|h(\vec{q})|^2\rangle$ [16]

$$\langle|h(\vec{q})|^2\rangle=\frac{A}{(2\pi)^5}\frac{w^2\zeta^2}{2}e^{-(4\pi^2+q^2\lambda^2)(\zeta^2/4\lambda^2)}I_o(\pi q\zeta^2/\lambda) \tag{6}$$

with $J_o(x)$ and $I_o(x)$, respectively, the Bessel and modified Bessel function of first kind and zero order. If $\zeta\gtrsim\lambda$ the surface is characteristic to that caused by the Schwoebel barrier effects [14], while for $\zeta\ll\lambda$ it reproduces behavior close to that of Gaussian roughness. Note that the correlation function $C(r)$ for mound roughness has an oscillatory behavior for $\zeta\gtrsim\lambda$ (strong Schwoebel barrier effect) leading to a characteristic satellite ring at $q=2\pi/\lambda$ of the power spectrum $\langle|h(\vec{q})|^2\rangle$ [16].

IV. RESULTS AND DISCUSSION

We should point out that the validity of Eq. (3) requires a weak roughness, such that $|\nabla h|<1$, or quantitatively small average local surface slopes $\rho_{\rm rms}=\sqrt{\langle|\nabla h|^2\rangle}$. Indeed, $\rho_{\rm rms}$ is given as a function of the roughness spectrum $\langle|h(\vec{q})|^2\rangle$ by the expression

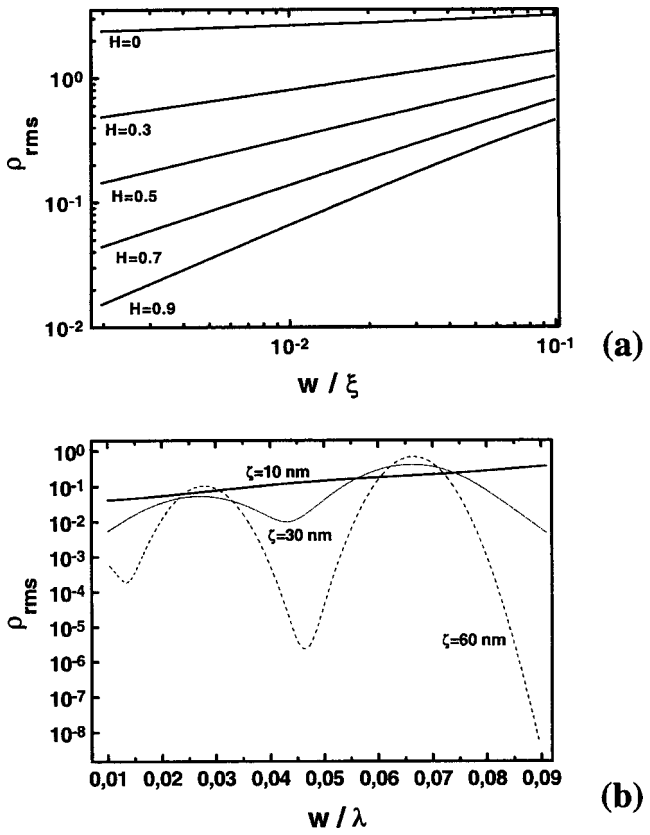

FIG. 1. (a) Local slope for self-affine roughness vs the roughness ratio w/ξ and various roughness exponents H as indicated. (b) Local slope for mound roughness vs roughness ratio w/λ for various system correlation lengths ζ as indicated.

$$\rho_{\rm rms}=\{[(2\pi)^4/A]\int_{0<q<Q_c} q^2\langle|h(\vec{q})|^2\rangle d^2q\}^{1/2}.$$

Figure 1 shows calculations of $\rho_{\rm rms}$ for both self-affine and mound roughness for roughness amplitudes $w=1$ nm and $c_o=0.3$ nm.

Furthermore, the equilibrium solid/liquid thicknesses (ℓ_s/ℓ_ℓ) are obtained by a minimization of $\Sigma(\ell_s,\ell_\ell)$ with respect to ℓ_s and ℓ_ℓ. The presence of the bending free energy $\Sigma_3(\ell_s)$ prevents complete wetting by a solid sheet, and imposes triple-point wetting (even for $S=0$) [12]. Minimization of $\Sigma(\ell_s,\ell_\ell)$ (far away from the triple point at solid-gas coexistence; $\ell_\ell=0$) yields $\partial\Sigma(\ell_s,\ell_\ell)/\partial\ell_s|_{\ell_\ell=0}=0$ or alternatively

$$\frac{\rho_s}{\rho_g}(P-P_o)-\frac{(C-\rho_s H)}{\ell_s^3}+\frac{3E}{2(1+v)}\frac{S^2}{\ell_s^2}\left(1+\frac{2S}{\ell_s}\right)$$

$$+\frac{E\ell_s^2}{8(1-v^2)}G=0. \qquad (7)$$

Equation (7) for negligible reduced stress or $S \ll \rho_s^2 C^2/E^2 G^{3/2}$ [12] and $P=P_o$ yields

$$\ell_s=[16\rho_s(1-v^2)]^{1/5}E^{-1/5}(C-\rho_s H)^{1/5}G^{-1/5}, \qquad (8)$$

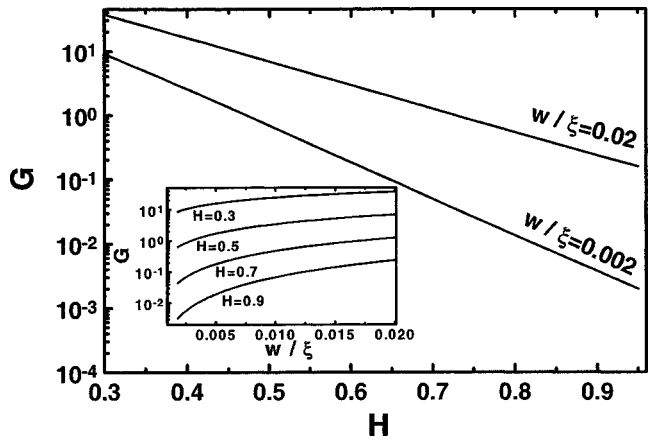

FIG. 2. Calculation of the factor G vs roughness exponent H for $w=1$ nm, $c_o=0.3$ nm, and various ratios w/ξ. The inset shows the factor G vs long wavelength roughness ratio w/ξ for $w=1$ nm ($w \ll \xi$), $c_o=0.3$ nm, and various roughness exponents H.

which shows a dependence of the layer thickness ℓ_s on the factor G as $\ell_s \propto G^{-1/5}$.

A. Self-affine roughness effects on factor G and solid layer thickness ℓ_s

Substitution of Eq. (5) into Eq. (4) yields for the factor G the simple analytic expression

$$G=\frac{w^2}{2a^3\xi^4}\left\{\frac{1}{2-H}[X_C^{2-H}-1]+\frac{2}{1-H}[1-X_C^{1-H}]\right.$$

$$\left.-\frac{1}{H}[X_C^{-H}-1]\right\} \qquad (9)$$

with $X_C=1+aQ_c^2\xi^2$. For $H=0$ and $H=1$, one has to employ the identity $\lim_{m\to 0}(1/m)[X_C^m-1]=\ln(X_c)$ to obtain the proper asymptotic form for the factor G. Figure 2 shows that the factor G increases with the increasing long wavelength roughness ratio w/ξ (indicating smoothing at large length scales $>\xi$), however, at a rate that strongly depends on the roughness exponent H. Indeed, G changes considerably with w/ξ (even by an order of magnitude) for large roughness exponents H (~ 1) as the inset indicates. Moreover, it becomes clear that as H changes within its physical range $0<H<1$ (to account for bounded roughness fluctuations), the factor G also changes significantly. The later implies that the short wavelength roughness fluctuations (as described by the roughness exponent H) will have a dominant influence on the factor G and thus on the solid wetting layer ℓ_ℓ.

Figure 3 shows the dependence of $\Lambda_s=\ell_s/[16\rho_s(1-v^2)]^{1/5}E^{-1/5}(C-\rho_s H)^{1/5}$ as a function of the roughness exponent H where it is clearly shown that ℓ_s will increase with increasing H and/or decreasing roughness ratio w/ξ (see also inset). In other words surface smoothing at any lateral length scale will favor a thicker solid film formation. This is in agreement with previous theoretical and experimental results by Esztermann *et al.* [12], where it was shown that the thickness of an adsorbed hydrogen layer (at solid-gas coex-

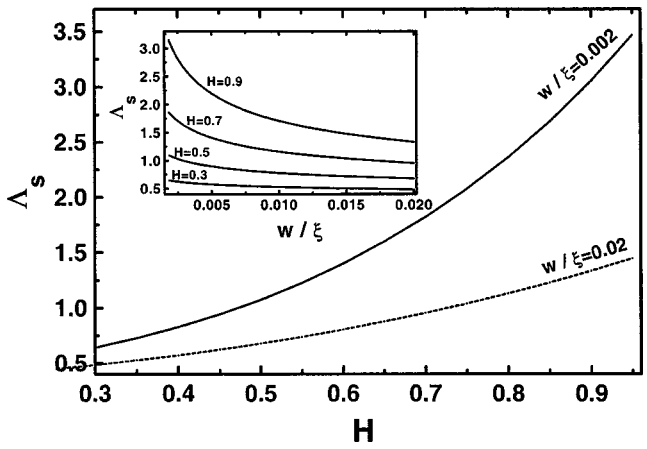

FIG. 3. Calculation of Λ_s vs roughness exponent H for $w=1$ nm, $c_o=0.3$ nm, and various ratios w/ξ. The inset shows calculations of Λ_s vs the roughness ratio w/ξ for various roughness exponents H, $w=1$ nm and $c_o=0.3$ nm.

istence) decreases with the increasing roughness factor G (increasing substrate roughness).

B. Mound roughness effects on factor G and solid layer thickness ℓ_s

Substitution of Eq. (6) into Eq. (4) yields the roughness factor G

$$G=\frac{w^2\zeta^2}{2}e^{-\pi\zeta^2/\lambda^2}\int_0^{Q_c}q^5e^{-q^2\zeta^2/4}I_o(\pi q\zeta^2/\lambda)dq, \quad (10)$$

where, upon extension of the integration to infinity, we obtain the analytic expression $G\cong 32(w^2/\zeta^4)e^{-2\pi\zeta^2/\lambda^2}[1-2\pi^2(\zeta^2/\lambda^2)+\pi^4(\zeta^4/2\lambda^4)]$. For $\zeta\ll\lambda$ (Gaussian roughness) the analytic expression for G yields $G\approx 32(w^2/\zeta^4)$, indicating that the influence of the average mound separation λ becomes negligible on the wetting scenario. In the more general case, the analytic calculation indicates that for mound roughness the factor G is proportional to the ratio w^2/ζ^4 while the average mound separation λ contributes mainly through the ratio ζ/λ.

In the following, the calculations of the factor G were performed in terms of Eq. (10). Figure 4 shows the factor G as a function of the average mound separation λ for various system correlation lengths ζ. The factor G decreases with increasing average mound separation λ in an oscillatory manner, and with oscillation amplitude which is amplified for small λ such that $\lambda<\zeta$. On the other hand, as a function of the system correlation length ζ, as the inset indicates, the factor G decreases at a rate that depends on the value of λ. The overall behavior is a complex function of both lateral roughness parameters λ and ζ, whose influence on the solid wetting layer ℓ_ℓ will be investigated in the following.

Figure 5 shows the dependence of $\Lambda_s=\ell_s/[16\rho_s(1-v^2)]^{1/5}E^{-1/5}(C-\rho_s H)^{1/5}$ as a function of the average mound separation λ. For small system correlation lengths ζ, the thickness increases with increasing average mound separation due to surface smoothing for decreasing roughness

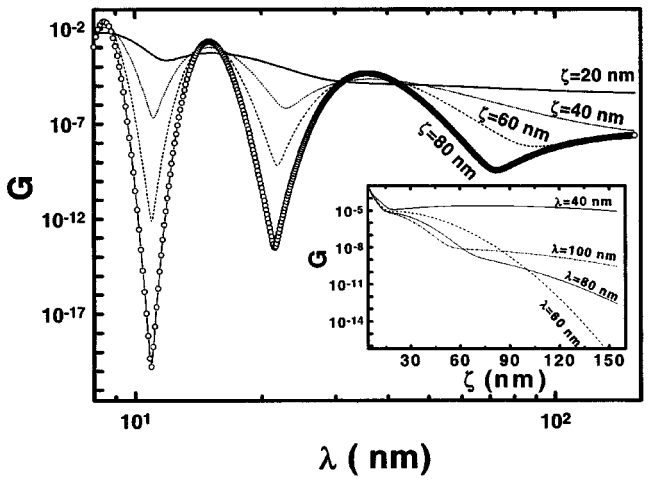

FIG. 4. Calculation of G vs average mound separation λ for $w=1$ nm, $c_o=0.3$ nm, and various system correlation lengths ζ. The inset shows calculations of G vs system correlation length ζ for various average mound separations λ, $w=1$ nm and $c_o=0.3$ nm.

ratio w/λ. However, the solid layer thickness increases in an oscillatory manner, with oscillation amplitude higher for the system correlation length ζ comparable to or larger than the average mound separation λ. As a function of the system correlation length ζ, the solid film thickness increases with increasing ζ or decreasing ratio w/ζ (surface smoothing) at a rate that depends on the value of λ as the inset indicates. As Fig. 5 indicates that with increasing roughness parameters λ and ζ (which leads to surface smoothing), the formation of thicker solid films will occur, however, with a thickness that strongly depends on the particular relative magnitude of ζ and λ.

V. CONCLUSIONS

We have shown the direct quantitative relation of characteristic self-affine and mound roughness parameters to triple-

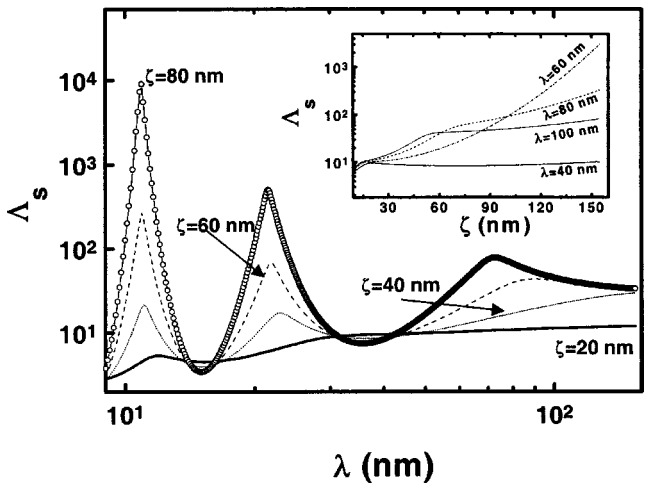

FIG. 5. Calculation of Λ_s vs average mound separation λ for $w=1$ nm, $c_o=0.3$ nm, and various system correlation lengths ζ. The inset shows calculations of Λ_s vs system correlation length ζ for various average mound separations λ, $w=1$ nm and $c_o=0.3$ nm.

wetting properties of solid films on rough substrates. With an increasing roughness exponent H and/or a decreasing ratio w/ξ, the thickness of adsorbed solid films on self-affine rough substrates increases noticeably in agreement also with recent studies [12]. For mound roughness the dependence on the lateral roughness parameters follows the general scenario that smoother substrates lead to thicker solid films, however, at a rate that depends on the relative magnitude of the roughness parameters ζ and λ. Therefore, a precise characterization of the substrate roughness is necessary in solid layer wetting situations (i.e., coatings of sculpted substrates, curved nanoparticles [22,23], etc.). Moreover, sufficiently smooth substrates will be necessary to produce adsorbed van der Waals film of significant thickness ($\geqslant$10 nm). This is of significant importance in diverse areas such as neutrino rest mass determination [24], laser fusion [25], slow muon surface investigations [26], and optical spectroscopy [27].

Finally we should point out that wetting studies that can make use of the previous calculations can, for example, be that of adsorption of hydrogen layers [12], on self-affine or mound rough substrates formed by nonequilibrium deposition of solid films (i.e., Au, Ag, Cu, etc.). Self-affine roughness can be formed by a deposition of metal films onto Si-oxide surfaces or other substrates at relatively low temperatures (i.e., close to room temperature) [13,14,28,29]. On the other hand, the growth of the mound roughness can be performed by the growth of Ag on Ag(111), Cu on Cu(001), Au on Au(001), and, in general, of metal overlayers on substrate surfaces with well-defined flat terraces separated by atomic steps, where the presence of Schwoebel barriers during the growth can lead to mound formation by inhibiting the diffusion of deposited adatoms across step edges [13–16,29]. Moreover, the variation of deposition parameters (deposition rate, substrate temperature, film thickness) can alter the solid thin film (substrate) roughness parameters [13–16,28,29], which, in turn, can be used as an alternative way to control the behavior of tripple-point wetting phenomena through variation of the substrate growth dynamics.

ACKNOWLEDGMENT

We would like to acknowledge support from the ''Nederlandse Organisatie voor Wetenschappelijk Onderzoek (NWO).''

[1] S. Dietrich, in *Phase Transitions and Critical Phenomena*, edited by C. Domb and J. Lebowitz (Academic, London, 1988), Vol. 12, pp. 1–128.
[2] R. Evans, in *Liquids at Interfaces*, Proceedings of the Les Houches Summer School, Session XLVIII, edited by J. Charvolin, J. F. Joanny, and J. Zinn-Justin (Elsevier, Amsterdam, 1990).
[3] H. Gau *et al.*, Science **283**, 46 (1999).
[4] K. Kargupta *et al.*, Phys. Rev. Lett. **86**, 4536 (2001).
[5] J. Bico *et al.*, Europhys. Lett. **47**, 220 (1999).
[6] S. Dietrich and M. Schick, Phys. Rev. B **33**, 4952 (1986).
[7] J. L. Seguin *et al.*, Phys. Rev. Lett. **51**, 122 (1983); M. Bienfait *et al.*, Phys. Rev. B **29**, 983 (1984); J. Krim, J. G. Dash, and J. Suzanne, Phys. Rev. Lett. **52**, 640 (1984).
[8] G. Mistura *et al.*, Phys. Rev. Lett. **82**, 795 (1999); L. Bruschi and G. Mistura, Phys. Rev. B **61**, 4941 (2000); J. Chem. Phys. **114**, 1350 (2001).
[9] Y. Qiao and H. K. Christenson, Phys. Rev. Lett. **83**, 1371 (1999).
[10] J. Klier *et al.*, Physica B **284**, 391 (2000).
[11] F. T. Gittes and M. Schick, Phys. Rev. B **30**, 209 (1984).
[12] A. Easztermann *et al.*, Phys. Rev. Lett. **88**, 055702 (2002).
[13] P. Meakin, Phys. Rep. **235**, 1991 (1994); J. Krim and G. Palasantzas, Int. J. Mod. Phys. B **9**, 599 (1995).
[14] P. Meakin, *Fractals, Scaling, and Growth far from Equilibrium* (Cambridge University Press, Cambridge, England, 1998); A.-L. Barabási and H. E. Stanley, *Fractal Concepts in Surface Growth* (Cambridge University Press, Cambridge, England, 1995); F. Family and T. Viscek, *Dynamics of Fractal Surfaces* (World Scientific, Singapore, 1991).
[15] M. D. Johnson, C. Orme, A. W. Hunt, D. Graff, J. Sudijono, L. M. Sander, and B. G. Orr, Phys. Rev. Lett. **72**, 116 (1994); M. Siegert and M. Plischke, *ibid.* **73**, 1517 (1994); J.-K. Zuo and J. F. Wendelken, *ibid.* **78**, 2791 (1997); J. A. Stroscio, D. T. Pierce, M. D. Stiles, A. Zangwill, and L. M. Sander, *ibid.* **75**, 4246 (1995).
[16] Y.-P. Zhao, H.-Y. Yang, G. C. Wang, and T.-M. Lu, Phys. Rev. B **57**, 1922 (1998).
[17] D. B. Pengra *et al.*, Surf. Sci. **245**, 125 (1991).
[18] Grain boundaries in the solid layer are neglected. However, local defect formation in the solid near the substrate interface is included since it will only alter the γ's. D. A. Huse, Phys. Rev. B **29**, 6985 (1984).
[19] L. D. Landau and E. M. Lifshitz, *Theory of Elasticity*, 3rd ed. (Pergamon, New York, 1986).
[20] M. Kardar and J. O. Indekeu, Europhys. Lett. **12**, 161 (1990); R. R. Netz and D. Andelman, Phys. Rev. E **55**, 687 (1997); G. Palasantzas, Phys. Rev. B **51**, 14612 (1995); G. Palasantzas and G. Backx, *ibid.* **55**, 9371 (1997).
[21] G. Palasantzas, Phys. Rev. B **48**, 14 472 (1993); **49**, 5785(E) (1994).
[22] C. Rascón and A. O. Parry, Nature (London) **407**, 986 (2000).
[23] M. Heni and H. Löwen, Phys. Rev. Lett. **85**, 3668 (2000).
[24] L. Fleischmann *et al.*, J. Low Temp. Phys. **119**, 615 (2000).
[25] R. S. Craxton *et al.*, Sci. Am. **255(2)**, 60 (1986).
[26] E. Morenzoni *et al.*, J. Appl. Phys. **81**, 3340 (1997).
[27] C. Bressler *et al.*, J. Chem. Phys. **105**, 10 178 (1996).
[28] G. Palasantzas and J. Krim, Phys. Rev. Lett. **73**, 3564 (1994); C. Thompson *et al.*, Phys. Rev. B **49**, 4902 (1994); P. Herrasti *et al.*, Phys. Rev. A **45**, 7440 (1992); R. C. Salvarezza *et al.*, Europhys. Lett. **20**, 727 (1992).
[29] Y. P. Zhao, G.-C. Wang, and T.-M. Lu, *Characterization of Amorphous and Crystalline Rough Surfaces—Principles and Applications*, Experimental Methods in the Physical Science Vol. 37 (Academic, New York, 2000). For mound roughness see also J. Vrijmoeth *et al.*, Phys. Rev. Lett. **72**, 3843 (1994).